# Exceptional Stationary State in a Dephasing Many-Body Open Quantum System

Alice Marché[1,*] Gianluca Morettini[1,*] Leonardo Mazza[1,2] Lorenzo Gotta[3] and Luca Capizzi[1]

[1]*Université Paris-Saclay, CNRS, LPTMS, 91405, Orsay, France*
[2]*Institut Universitaire de France, 75005 Paris, France*
[3]*Department of Quantum Matter Physics, University of Geneva, 1211 Geneva, Switzerland*

We study a dephasing many-body open quantum system that hosts, together with the infinite-temperature state, another additional stationary state, that is associated with a nonextensive strong symmetry. This state, that is a pure dark state, is exceptional in that it retains memory of the initial condition, whereas any orthogonal state evolves toward the infinite-temperature state erasing any information on the initial state. We discuss the approach to stationarity of the model focusing in particular on the fate of interfaces between the two states. A simple model based on a membrane picture helps developing an effective large-scale theory, which is different from the usual hydrodynamics since no extensive conserved quantities are present. The fact that the model reaches stationary properties on timescales that diverge with the system size, while the Lindbladian gap is finite, is duly highlighted. We point out the reasons for considering these exceptional stationary states as quantum many-body scars in the open system framework.

*Introduction*—The eigenstate thermalization hypothesis (ETH) stands as a cornerstone in condensed-matter physics, as it describes in simple and physical terms the emergence of thermal features in the late-time dynamics of closed quantum systems [1–5]. In the last years, exceptional dynamics that escape thermalization by retaining memory of the initial conditions have been identified as a primary mechanism for violating the ETH, via rare eigenstates dubbed many-body quantum scars [6–11]. The broad goal of this Letter is to study a similar phenomenon in Markovian many-body open quantum systems (MBOQS) [12,13], discussing a specific dephasing model.

The late-time behavior of Markovian MBOQS [14,15] has recently attracted a great deal of attention [16–23]. In the absence of any strong symmetry [24,25], one generically expects a unique stationary state that is progressively approached from any initial state. This leads to the complete erasure of any information on the initial state, a behavior that resembles closely the ergodicity that always accompanies thermalization in closed systems. Whether a MBOQS could also withstand an exceptional stationary state is something that has not been discussed yet.

In this Letter we study a one-dimensional dephasing model where the infinite-temperature (mixed) state and the fully polarized (pure) state are the only stationary states. The latter is a dark state of the model, but we argue that additionally it plays the role of a scar in this MBOQS because it is not protected by *extensive* strong symmetries

[26]. In fact, it is protected by a *nonextensive* symmetry: no spatial density of conserved quantity exists that could give rise to transport phenomena. Given that we can also demonstrate the presence of a finite spectral gap of the Lindbladian, these considerations rule out the presence of hydrodynamic slow modes. Nonetheless, we show that the interface between the two stationary states diffuses according to the physics of a fluctuating membrane, in a scenario characterized by long relaxation times, and we show how it is consistent with the finite Lindbladian gap (see also [27–30]).

*The model*—We consider a one-dimensional spin-1/2 chain of length $L$ whose density matrix $\rho$ evolves according to the Lindblad master equation

$$\frac{d}{dt}\rho = \mathcal{L}[\rho] = -i[H,\rho] + \sum_j L_j \rho L_j^\dagger - \frac{1}{2}\{L_j^\dagger L_j, \rho\}, \quad (1)$$

with jump operators $L_j = \sqrt{\gamma}\sigma_j^z$ and Hamiltonian

$$H = \sum_j J[\sigma_j^+ \sigma_{j+1}^- + \text{H.c.}] + g[\sigma_j^x \pi_{j+1}^z + \pi_j^z \sigma_{j+1}^x], \quad (2)$$

where $\pi_j^\alpha = \mathbb{1} - \sigma_j^\alpha$, for $\alpha = x, y, z$. Here, $J$ is the strength of the nearest-neighbor hopping term, while $g$ multiplies the East-West Hamiltonian [31], according to which a spin can be flipped only when a neighboring spin is in a $|\downarrow\rangle$ state. The dissipation occurs at a rate $\gamma$ and it is associated with the decay of coherence in the $z$-polarized basis; as such it is naturally interpreted as a *dephasing* process.

For $g = 0$ the model can be solved analytically with Bethe-ansatz techniques [32], and, unless otherwise specified, we focus here on $g, J \neq 0$.

*Stationary states*—The infinite temperature state $\rho_\infty = \mathbb{1}/\text{Tr}[\mathbb{1}]$ is a stationary state of (1), as a consequence of $L_j = L_j^\dagger$. Furthermore, given the specific choice of the Hamiltonian and dissipation the pure state $\rho_\Uparrow = |\Uparrow\rangle\langle\Uparrow|$ associated with all spins aligned along the $z$ axis, is also stationary and is a dark state of the model [33]. Note that the two states are not orthogonal according to the Hilbert-Schmidt scalar product $\langle \rho, \tau \rangle_{\text{HS}} := \text{Tr}[\rho^\dagger \tau]$ because $\langle \rho_\Uparrow, \rho_\infty \rangle_{\text{HS}} = 2^{-L}$; hence it is convenient to consider $\rho'_\infty := (\mathbb{1} - \rho_\Uparrow)/\text{Tr}[\mathbb{1} - \rho_\Uparrow]$, which is orthogonal to $\rho_\Uparrow$ but whose local properties differ from those of $\rho_\infty$ by a term that is exponentially small in the system size.

We point out that $\rho_\Uparrow$ is technically a strong symmetry (i.e., a conserved quantity of the MBOQS [24,25]) of the model, meaning that it commutes with both $H$ and $L_j$ $\forall$ $j$; nonetheless, since it cannot be written as $\sum_j q_j$, with $q_j$ a local operator, it is nonextensive. When $g = 0$, instead, the total magnetization is an *extensive* strong symmetry.

No additional states are stationary. To prove that, we consider the Lindbladian $\mathcal{L}$, which is a linear non-Hermitian superoperator, and study its complex spectrum, plotted in Fig. 1(a), obtained with the exact-diagonalization (ED) of a spin chain of size $L = 6$. The calculation is performed with the open-source Python-framework QuTiP [34,35]. The inset shows that the eigenvalue $\lambda = 0$ is two-fold degenerate, and we have checked that the two associated eigenvectors can be identified with $\rho_\infty$ and $\rho_\Uparrow$. This feature is compatible with properties of the commutant algebra [21,26,36,37] of the model, derived in the End Matter (EM) and detailed in Supplemental Material (SM) [38].

The numerics allows us also to conclude that the Lindbladian spectral gap, $\Delta = \min_{\lambda \neq 0}|\text{Re}[\lambda]|$ does not close with system size, and specifically that it has a large-$L$ scaling $\Delta(L) \simeq \Delta_0 + (\Delta_1/L^2)$ with $\Delta_0 \neq 0$ whenever $g \neq 0$. [We remark that, at $g = 0$ the degeneracy of the eigenvalue $\lambda = 0$ is enhanced, due to the $U(1)$ symmetry associated with the conservation of the magnetization along the $z$ axis.] The numerical scaling of $\Delta(L)$ is presented in Fig. 1(b) for sizes up to $L = 12$. The specific value of $\Delta_0$ depends on the choice of open versus periodic boundary conditions; see EM.

*Dynamics*—We argue that any initial pure state $|\psi\rangle$ that is orthogonal to $|\Uparrow\rangle$ must relax eventually toward $\rho'_\infty$. The approach to $\rho'_\infty$ can be quantified by the normalized Hilbert-Schmidt scalar product

$$\theta'_\infty(t) := \frac{\text{Tr}[\rho'_\infty \rho(t)]}{\sqrt{\text{Tr}[\rho'^2_\infty]\text{Tr}[\rho(t)^2]}} \qquad (3)$$

that generalizes the scalar product $|\langle \psi | \psi' \rangle|^2$ (which holds for pure states). Since $\rho'_\infty$ and $\rho(t)$ are positive and
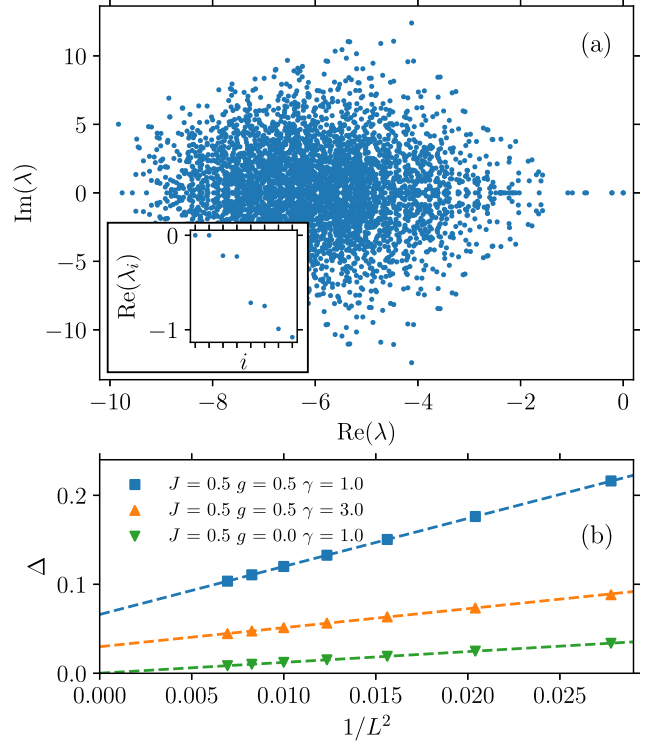


FIG. 1. (a) Lindbladian spectrum for the following parameters: $[J, g, \gamma, L] = [0.5, 0.5, 1, 6]$. Inset: real parts of the eigenvalues closest to zero, labeled by the index $i$. (b) Lindbladian gap $\Delta$ as a function of $1/L^2$ for $L \in \{6, ..., 12\}$. The results are compatible with a scaling $\Delta(L) = \Delta_0 + \Delta_1/L^2 + o(L^{-2})$. The three curves correspond to different sets of parameters: $[J, g, \gamma] = [0.5, 0.5, 1]$, $[0.5, 0.5, 3]$, or $[0.5, 0, 1]$. For both panels (a) and (b), open boundary conditions are considered.

Hermitian operators, $\theta'_\infty(t) \geq 0$. Moreover, by the Cauchy-Schwartz inequality $\theta'_\infty(t) \leq 1$ and $\theta'_\infty(t) = 1$ if and only if $\rho(t) \equiv \rho'_\infty$ in particular, whenever $\langle \psi | \Uparrow \rangle = 0$, $\theta'_\infty(t)$ is expected to converge to 1 at sufficiently large time $t$.

We employ the ITensor Julia library [41,42] and develop a tensor-network representation of the density matrices $\rho'_\infty$ and $\rho(t)$, where the latter is computed with an algorithm based on the time-dependent variational principle [43,44] that integrates the dynamics (1); see EM for details. The scalar product $\theta'_\infty(t)$ can be efficiently computed and we can study chains of length $L = 40$.

Our results are plotted in Fig. 2(a) and demonstrate the time-evolution towards $\rho'_\infty$ of three initial states orthogonal to $|\Uparrow\rangle$, namely the fully-polarized state $|\Downarrow\rangle$ with all spins in the $|\downarrow\rangle$ state, the antiferromagnetic Néel state $|\text{Néel}\rangle = |\uparrow\downarrow\uparrow\downarrow\uparrow\downarrow...\rangle$, and the state $|\uparrow\downarrow\downarrow\downarrow\uparrow\downarrow\downarrow\downarrow...\rangle$. We also verified numerically the fact that $|\Uparrow\rangle$ is stationary and retains $\theta'_\infty(t) = 0$ at all times.

These results highlight the separation of the Hilbert space into two disconnected subspaces. On the one hand, we have the state $|\Uparrow\rangle$ and the associated subspace $\mathcal{S}_\Uparrow$. On the other hand, the subspace $\mathcal{T}_\Uparrow$, orthogonal to $\mathcal{S}_\Uparrow$, is
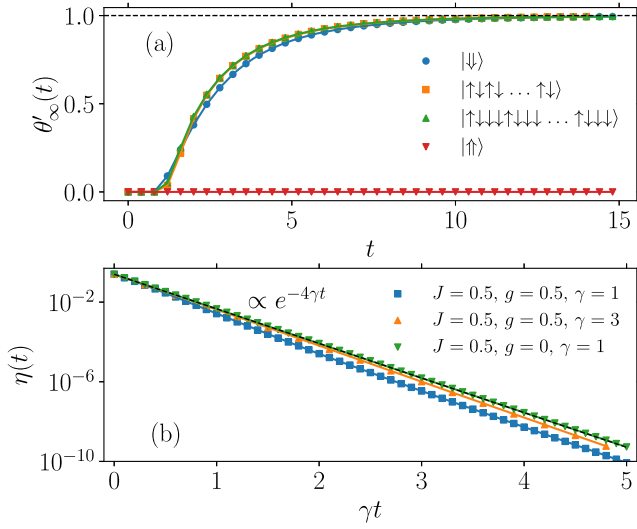
FIG. 2. (a) Time evolution of $\theta'_\infty(t)$ for the initial states $|\Downarrow\rangle$, $|\text{Néel}\rangle$, $|\uparrow\downarrow\downarrow\uparrow\downarrow\downarrow\ldots\rangle$, and $|\Uparrow\rangle$. The parameters are $[J, g, \gamma, L] = [0.5, 0.5, 1, 40]$. (b) Time evolution of $\eta(t)$ for the initial state $|\uparrow\ldots\uparrow \to \uparrow\ldots\uparrow\rangle$. We observe that the upper bound is saturated for $g = 0$.

characterized by a loss of information on the initial conditions, and an eventual relaxation towards $\rho'_\infty$.

We now show that any coherence between the two subspaces $\mathcal{T}_\Uparrow$ and $\mathcal{S}_\Uparrow$ is lost exponentially in time by introducing the quantifier

$$\eta(t) := \sum_{|\boldsymbol{\sigma}\rangle \neq |\Uparrow\rangle} |\langle\boldsymbol{\sigma}|\rho(t)|\Uparrow\rangle|^2, \tag{4}$$

where $\{|\boldsymbol{\sigma}\rangle\}$ is a basis for the Hilbert space of the entire spin chain composed of states that are simultaneous eigenstates of all $\sigma_j^z$; the sum is restricted over a basis of $\mathcal{T}_\Uparrow$. With a few simple algebraic passages, we obtain the following suggestive rewriting: $\eta(t) = \langle\Uparrow|\rho(t)^2|\Uparrow\rangle - \langle\Uparrow|\rho(t)|\Uparrow\rangle^2$, which proposes the simple interpretation of $\eta(t)$ as the variance of the operator $\rho(t)$ on the state $|\Uparrow\rangle$, and proves that the definition of $\eta(t)$ is basis independent. By definition, $0 \leq \eta(t) \leq 1$.

In the EM, we detail a few algebraic passages that demonstrate the inequality $(d/dt)\eta(t) \leq -4\gamma\eta(t)$, and thus that $\eta(t) \leq \eta(0)e^{-4\gamma t}$, proving an exponential decay in time of the coherence between the two subspaces associated with the two different dynamics. We explicitly verified this prediction on a system initialized in the state $|\uparrow\ldots\uparrow \to \uparrow\ldots\uparrow\rangle$, $\to$ denoting the spin aligned along the $x$ axis; see Fig. 2(b).

*Open-system quantum many-body scars*—The results presented so far motivate the interpretation of $|\Uparrow\rangle$ as an *open-system generalization of isolated quantum many-body scars* [31,45], as we are now going to explain.

We first remark that, in general, many-body systems can possess extensive conserved quantities generated by local

densities, $Q_a = \sum_j q_{a,j}$. For closed systems, the (generalized) Gibbs ensembles $\langle\ldots\rangle \propto \text{Tr}[e^{-\sum_a \beta_a Q_a} \ldots]$ are the stationary states determined the $Q_a$s. They are crucial for the appearance of a standard hydrodynamic behavior, based on the description of the system in terms of local Gibbs ensembles [46–48], with $\beta_a(x, t)$ depending smoothly on coarse-grained spatial and time variables. According to strong ETH, these are the only possible stationary states [3,4]; in particular, when only $H$ is conserved, the eigenstates of the Hamiltonian are expected to be locally indistinguishable from Gibbs ensembles at the corresponding energy density. Violations of such a scenario are possible, for instance, via the presence of eigenstates whose local properties are not described by Gibbs ensembles, and are dubbed *quantum many-body scars* [9–11]. These states are associated to nonextensive symmetries [26].

Following this analogy, we propose to identify scars in MBOQS characterized by dephasing jump operators as *stationary states that are not protected by extensive conserved operators*. We have already seen that when $g \neq 0$, $|\Uparrow\rangle\langle\Uparrow|$ is a conserved operator (strong-symmetry) which is not extensive [45]: we identify $|\Uparrow\rangle$ as an *open system quantum many-body scar*. In contrast, for $g = 0$ the conservation of the magnetization $S^z$, which is extensive, protects $|\Uparrow\rangle$, and we refrain from calling it scar: it would just be a dark state. Moreover, the absence of extensive conserved operators rules out the existence of a standard late-time hydrodynamics and of its slow modes; this is compatible with the accepted expectation that the finite Lindbladian spectral gap plotted in Fig. 1(b) should force a relaxation on a finite timescale in the thermodynamic limit (note instead that for $g = 0$ the gap is zero, compatibly with the hydrodynamics of $S^z$).

Finally, we point out that a rigorous and widely accepted definition of scars in MBOQS is, up to our knowledge, absent, and different points of view on weak ergodicity breaking in open quantum systems have been proposed in Refs. [49–53].

*Membrane diffusion of the interface*—We now discuss the existence of slow decay modes also in model (1), notwithstanding the finite spectral gap and the absence of hydrodynamics. We consider a bipartition protocol where we juxtapose the infinite temperature state and the scar (on the left/right half chain, respectively): with a slight abuse of notation, we denote the initial state as $\rho(0) = \rho_\infty \otimes \rho_\Uparrow$. We show the numerical results for the local magnetization $\langle\sigma_j^z(t)\rangle := \text{Tr}[\sigma_j^z\rho(t)]$ in Fig. 3, displaying a progressive melting of the scar, as expected for the eventual thermalization. However, the picture suggests that thermalization is slowly achieved on a time-scale diverging as $L$; while the diffusive broadening resembles standard hydrodynamics, we have ruled out such scenario. We instead propose a *membrane picture* [54,55] to describe the fluctuating dynamics of the interface separating the two stationary states.
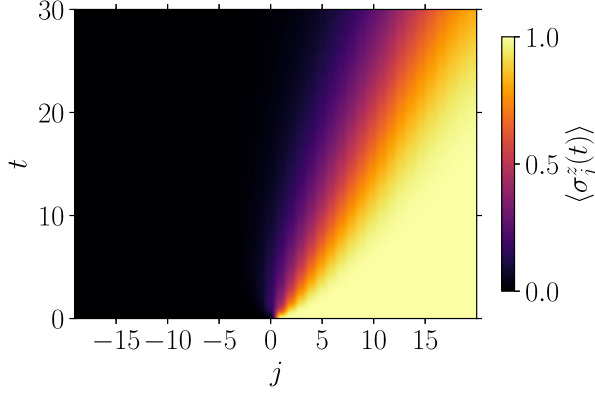
FIG. 3. Magnetization profile $\langle \sigma_j^z(t) \rangle$ as a function of $j$ and $t$. The initial state is obtained by joining the infinite-temperature state, with support $j \in [-L/2 + 1, 0]$, and the full-aligned up state along the $z$ axis elsewhere. The evolution is performed for the model in Eq. (1) with the following parameters: $[J, g, \gamma, L] = [0.5, 0.5, 1, 40]$.

We are able to pinpoint analytically this picture in the large-$\gamma$ limit of the dynamics (1) using the second-order perturbation theory for $g/\gamma$, $J/\gamma \ll 1$ introduced in Ref. [18] for dephasing models. It is based on an effective Lindbladian $\mathcal{L}_{\text{eff}}$ that acts onto the states $\rho_{\boldsymbol{\sigma}} = |\boldsymbol{\sigma}\rangle\langle\boldsymbol{\sigma}|$, which are easily proven to be the only stationary states for $g, J = 0$ and thus determine the late-time dynamics $t \gg \gamma^{-1}$ whenever $g/\gamma$, $J/\gamma \ll 1$.

The action of $\mathcal{L}_{\text{eff}}$ onto a density matrix $\rho(t) = \sum_{\boldsymbol{\sigma}} p_{\boldsymbol{\sigma}}(t)|\boldsymbol{\sigma}\rangle\langle\boldsymbol{\sigma}|$, is most easily described using the Doi-Peliti formalism that represents the density matrix $\rho(t)$ as a vector $|\rho(t)\rangle = \sum_{\boldsymbol{\sigma}} p_{\boldsymbol{\sigma}}(t)|\boldsymbol{\sigma}\rangle$ that satisfies the unconventional normalization condition $\sum_{\boldsymbol{\sigma}} p_{\boldsymbol{\sigma}} = 1$ [56,57]. The Lindblad dynamics $(d/dt)\rho(t) = \mathcal{L}_{\text{eff}}[\rho(t)]$ is translated into the form $(d/dt)|\rho(t)\rangle = -W|\rho(t)\rangle$ with the Markov generator (see EM and SM [38])

$$W = -\frac{J^2}{4\gamma}\sum_j (\sigma_j^x \sigma_{j+1}^x + \sigma_j^y \sigma_{j+1}^y + \sigma_j^z \sigma_{j+1}^z - 1)$$
$$+ 2\frac{g^2}{\gamma}\sum_j (\pi_j^x \pi_{j+1}^z + \pi_{j+1}^x \pi_j^z + \pi_{j-1}^z \pi_j^x \pi_{j+1}^z). \quad (5)$$

Since the dynamics induced by $W$ cannot be determined analytically, we propose a simplified but analytically tractable generator $\tilde{W} = W - 2(g^2/\gamma)\sum_j \pi_{j-1}^z \pi_j^x \pi_{j+1}^z$ without terms coupling three sites. We also make a specific choice of the parameters, namely, $J^2/4\gamma = 1/6$ and $2g^2/\gamma = 1/6$: this allows us to provide rigorous estimates for the spectral gap (see SM [38]) and exact calculations for the interface dynamics.

We introduce the vector $|\bullet\rangle = \frac{1}{2}(|\uparrow\rangle + |\downarrow\rangle)$, namely, the local infinite temperature state, and we define the state $|x\rangle \equiv |\bullet \ldots \bullet\bullet\underset{x}{\uparrow}\uparrow\ldots\uparrow\rangle$, representing an interface between the positions $x$ and $x + 1$. The states $|x\rangle$ are the essence

of the membrane picture. By explicit computation, $\tilde{W}|x\rangle = |x\rangle - \frac{2}{3}|x + 1\rangle - \frac{1}{3}|x - 1\rangle$, and therefore the space of single domain-wall states is closed under Markov dynamics; in particular, the evolution reduces to a one-dimensional Brownian motion with drift on the lattice, which can be solved exactly using the Fourier transform. The explicit solution is $|\rho(t)\rangle = e^{-\tilde{W}t}|x=0\rangle = \sum_x p(x,t)|x\rangle$ with $p(x,t) \equiv \int_{-\pi}^{\pi}(dk/2\pi)\exp(-\varepsilon(k)t + ikx)$, where $\varepsilon(k) = 1 - \cos(k) + (i/3)\sin k$. Here, $p(x,t)$ is the probability distribution of the domain-wall position; in the large $t$ limit, we approximate it as

$$p(x,t) \simeq \frac{1}{\sqrt{2\pi\mathcal{D}t}}\exp\left(-\frac{(x - vt)^2}{2\mathcal{D}t}\right), \quad (6)$$

where $v = 1/3$ and $\mathcal{D} = 1$, the *drift velocity* and the *diffusion constant*, respectively, are defined by the small $k$ expansion $\varepsilon(k) \simeq ivk + \frac{1}{2}\mathcal{D}k^2 + O(k^3)$.

The expectation value of the local magnetization operator $\sigma_j^z$ plotted in Fig. 3 has a simple representation using membrane states, $\langle \sigma_j^z(t) \rangle = \sum_{j' < j} p(j', t)$; in the large-scale coarse-grained limit where the discrete lattice site $j$ is replaced by a continuous variable $x$, it can be approximated by the error function

$$\langle \sigma^z(x, t) \rangle \simeq \int_{-\infty}^{\frac{x-vt}{\sqrt{\mathcal{D}t}}} \frac{du}{\sqrt{2\pi}}\exp\left(-\frac{u^2}{2}\right). \quad (7)$$

In general, at late times, we can interpret the local state across the interface as a statistical mixture of the two stationary states.

In Fig. 4 we show that the membrane picture gives an accurate description of the dynamics and show that the interface is actually evolving via a diffusive broadening with drift, even if we are not in the large-dissipation limit of the analytical picture and we simulate the full Lindbladian. The collapse of the data presented in Fig. 3 against the rescaled variable $(x - vt)/\sqrt{\mathcal{D}t}$, where $v$ and $\mathcal{D}$ have been fitted, is excellent. In order to show that this behavior is not a peculiar feature of our model, in the SM [38] we present numerical simulations for the other two models.

*Late-time asymptotics and spectral gap*—We conclude by reconcyling the slow dynamics we just computed with the presence of a finite Lindbladian gap $\Delta_0$, following a reasoning that is reminiscent of Ref. [29]. In general, $\Delta_0$ is interpreted as a finite asymptotic decoherence rate [14,15], or, equivalently, as a typical timescale $\tau_0 \sim 1/\Delta_0$ that does not depend on the system size and that gives an upper bound to the time that is necessary for the system to reach stationarity. On the contrary, our numerics in Fig. 3 and the membrane analytical picture show that the thermalization of the interface requires a timescale that necessarily grows with the size of the system ($v$ and $\mathcal{D}$ are finite in the thermodynamic limit). This suggests that the identification
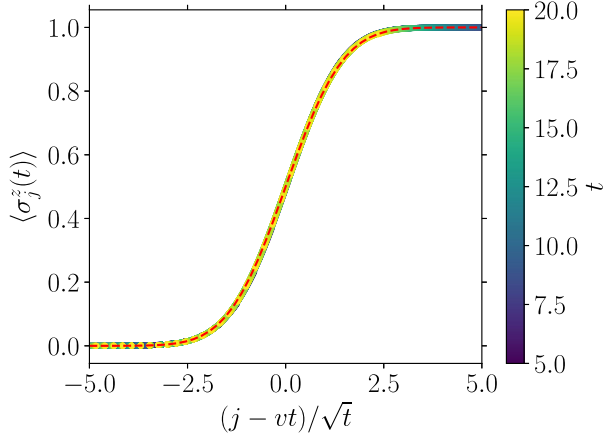
FIG. 4. Profile of the magnetization shown in Fig. 3 as a function of the scaling variable $(j - vt)/\sqrt{t}$. The rescaled data collapse onto the universal function described by Eq. (7), represented by the red dashed line. The velocity $v$ is determined by interpolating numerically, at each time $t$, the position $x$ where the profile satisfies $\langle \sigma_j^z(t) \rangle = 0.5$. The diffusion constant $\mathcal{D}$ is a fit parameter. Here, $v \simeq 0.453$ and $\mathcal{D} \simeq 1.33$. Parameters used: $[J, g, \gamma, L] = [0.5, 0.5, 1, 40]$.

of the bona fide asymptotic decay rate in a MBOQS requires a careful study not only of the Lindbladian spectral properties, but also of the size-dependence of the decomposition of initial states onto the eigenvectors of the Lindbladian [27–30].

To do so, we investigate the finite-size behavior of the interface dynamics; specifically, we focus on the spectral properties of the Markov operator $\tilde{W}$ with open boundary conditions. We express the evolution of a local observable $\mathcal{O}$, with $|x_0\rangle$ the initial interface state, as

$$\langle \mathcal{O}(t) \rangle - \langle \mathcal{O}(t = \infty) \rangle = \sum_{n \neq 0} e^{-\epsilon_n t}(\mathbb{1}|\mathcal{O}|n)(\tilde{n}|x_0). \quad (8)$$

Here, $\epsilon_n$ are the eigenvalues of $\tilde{W}$, $\{|n)\}_n$, $\{(\tilde{n}|\}_n$ its right/left eigenvectors respectively [58] and $(\mathbb{1}| := \sum_\sigma (\sigma|$. We checked that the matrix $\tilde{W}$ has a real spectrum even if it is nonsymmetric, and its nonzero eigenvalues are separated by a finite gap $\Delta$. As a consequence, we estimate an eventual exponential decay of (8) via

$$|\langle \mathcal{O}(t) \rangle - \langle \mathcal{O}(t = \infty) \rangle| \leq e^{-\Delta t} \sum_{n \neq 0} |(\mathbb{1}|\mathcal{O}|n)(\tilde{n}|x_0)|. \quad (9)$$

However, the magnitude of the matrix elements appearing above grows exponentially in the system size as $|(\mathbb{1}|\mathcal{O}|n)(\tilde{n}|x_0)| \sim e^{O(L)}$ in a phenomenology related to that of the *non-Hermitian skin effect* [59] (details are in the EM). As a consequence, the bound (9) can only be useful for timescales $t \gtrsim L$ and is otherwise too loose. This explains the apparent discrepancy between the spectral gap and the relaxation time of local observables.

*Conclusions*—We have discussed a MBOQS dephasing model with an exceptional stationary state $|\Uparrow\rangle$ that retains the memory of the initial condition while any other initial state relaxes toward the infinite-temperature state $\rho'_\infty$. We have employed this model to stress a viewpoint on quantum many-body scars in open systems based on the absence of extensive strong symmetries and of the associated longtime hydrodynamics. Nonetheless, the scar is proven responsible for a slow-relaxation phenomenon that is based on the membrane diffusion mechanism. The Letter opens the path toward the study of dynamics in the presence of exceptional stationary states, the universal features of the longtime dynamics, and their relation with the spectral properties of the Lindbladian [13,60,61].

*Data availability*—The data that support the findings of this article are not publicly available upon publication because it is not technically feasible and/or the cost of preparing, depositing, and hosting the data would be prohibitive within the terms of this research project. The data are available from the authors upon reasonable request.

[1] Michael V. Berry, Regular and irregular semiclassical wavefunctions, J. Phys. A **10**, 2083 (1977).

[2] Josh M. Deutsch, Quantum statistical mechanics in a closed system, Phys. Rev. A **43**, 2046 (1991).

[3] Mark Srednicki, The approach to thermal equilibrium in quantized chaotic systems, J. Phys. A **32**, 1163 (1999).

[4] Luca D'Alessio, Yariv Kafri, Anatoli Polkovnikov, and Marcos Rigol, From quantum chaos and eigenstate thermalization to statistical mechanics and thermodynamics, Adv. Phys. **65**, 239 (2016).

[5] Silvia Pappalardi, Laura Foini, and Jorge Kurchan, Eigenstate thermalization hypothesis and free probability, Phys. Rev. Lett. **129**, 170603 (2022).

[6] Hannes Bernien, Sylvain Schwartz, A. Keesling, H. Levine, Ahmed Omran, Hannes Pichler, Soonwon Choi, A. S. Zibrov, Manuel Endres, Markus Greiner, Vladan Vuletić, and Mikhail D. Lukin, Probing many-body dynamics on a 51-atom quantum simulator, Nature (London) **551**, 579 (2017).

[7] C. J. Turner, A. A. Michailidis, D. A. Abanin, M. Serbyn, and Z. Papić, Weak ergodicity breaking from quantum many-body scars, Nat. Phys. **14**, 745 (2018).

[8] Daniel K. Mark and Olexei I. Motrunich, $\eta$-pairing states as true scars in an extended Hubbard model, Phys. Rev. B **102**, 075132 (2020).

[9] Maksym Serbyn, Dmitry A. Abanin, and Zlatko Papić, Quantum many-body scars and weak breaking of ergodicity, Nat. Phys. **17**, 675 (2021).

[10] Sanjay Moudgalya, B. Andrei Bernevig, and Nicolas Regnault, Quantum many-body scars and Hilbert space fragmentation: A review of exact results, Rep. Prog. Phys. **85**, 086501 (2022).

[11] Anushya Chandran, Thomas Iadecola, Vedika Khemani, and Roderich Moessner, Quantum many-body scars: A quasiparticle perspective, Annu. Rev. Condens. Matter Phys. **14**, 443 (2023).

[12] Rosario Fazio, Jonathan Keeling, Leonardo Mazza, and Marco Schiro, Many-body open quantum systems, arXiv:2409.10300.

[13] Lukas M. Sieberer, Michael Buchhold, Jamir Marino, and Sebastian Diehl, Universality in driven open quantum matter, Rev. Mod. Phys. **97**, 025004 (2025).

[14] E. M. Kessler, G. Giedke, A. Imamoglu, S. F. Yelin, M. D. Lukin, and J. I. Cirac, Dissipative phase transition in a central spin system, Phys. Rev. A **86**, 012116 (2012).

[15] Fabrizio Minganti, Alberto Biella, Nicola Bartolo, and Cristiano Ciuti, Spectral theory of Liouvillians for dissipative phase transitions, Phys. Rev. A **98**, 042118 (2018).

[16] Dario Poletti, Jean-Sébastien Bernier, Antoine Georges, and Corinna Kollath, Interaction-induced impeding of decoherence and anomalous diffusion, Phys. Rev. Lett. **109**, 045302 (2012).

[17] Dario Poletti, Peter Barmettler, Antoine Georges, and Corinna Kollath, Emergence of glasslike dynamics for dissipative and strongly interacting bosons, Phys. Rev. Lett. **111**, 195301 (2013).

[18] Zi Cai and Thomas Barthel, Algebraic versus exponential decoherence in dissipative many-particle systems, Phys. Rev. Lett. **111**, 150403 (2013).

[19] Raphaël Bouganne, Manel Bosch Aguilera, Alexis Ghermaoui, Jérôme Beugnon, and Fabrice Gerbier, Anomalous decay of coherence in a dissipative many-body system, Nat. Phys. **16**, 21 (2019).

[20] D. Wellnitz, G. Preisser, V. Alba, J. Dubail, and J. Schachenmayer, Rise and fall, and slow rise again, of operator entanglement under dephasing, Phys. Rev. Lett. **129**, 170401 (2022).

[21] Yahui Li, Pablo Sala, and Frank Pollmann, Hilbert space fragmentation in open quantum systems, Phys. Rev. Res. **5**, 043239 (2023).

[22] Pietro Brighi and Marko Ljubotina, Anomalous transport in the kinetically constrained quantum east-west model, Phys. Rev. B **110**, L100304 (2024).

[23] Yahui Li, Frank Pollmann, Nicholas Read, and Pablo Sala, Highly-entangled stationary states from strong symmetries, Phys. Rev. X **15**, 011068 (2025).

[24] Berislav Buča and Tomaž Prosen, A note on symmetry reductions of the Lindblad equation: Transport in constrained open spin chains, New J. Phys. **14**, 073007 (2012).

[25] Victor V. Albert and Liang Jiang, Symmetries and conserved quantities in Lindblad master equations, Phys. Rev. A **89**, 022118 (2014).

[26] Sanjay Moudgalya and Olexei I. Motrunich, Exhaustive characterization of quantum many-body scars using commutant algebras, Phys. Rev. X **14**, 041069 (2024).

[27] Marko Žnidarič, Relaxation times of dissipative many-body quantum systems, Phys. Rev. E **92**, 042143 (2015).

[28] Takashi Mori and Tatsuhiko Shirai, Resolving a discrepancy between Liouvillian gap and relaxation time in boundary-dissipated quantum many-body systems, Phys. Rev. Lett. **125**, 230604 (2020).

[29] Taiki Haga, Masaya Nakagawa, Ryusuke Hamazaki, and Masahito Ueda, Liouvillian skin effect: Slowing down of relaxation processes without gap closing, Phys. Rev. Lett. **127**, 070402 (2021).

[30] Tibor Rakovszky, Sarang Gopalakrishnan, and Curt von Keyserlingk, Defining stable phases of open quantum systems, Phys. Rev. X **14**, 041031 (2024).

[31] Nicola Pancotti, Giacomo Giudice, J. Ignacio Cirac, Juan P. Garrahan, and Mari Carmen Bañuls, Quantum east model: Localization, nonthermal eigenstates, and slow dynamics, Phys. Rev. X **10**, 021051 (2020).

[32] Mariya V. Medvedyeva, Fabian H. L. Essler, and Tomaž Prosen, Exact Bethe ansatz spectrum of a tight-binding chain with dephasing noise, Phys. Rev. Lett. **117**, 137202 (2016).

[33] B. Kraus, H. P. Büchler, S. Diehl, A. Kantian, A. Micheli, and P. Zoller, Preparation of entangled states by quantum Markov processes, Phys. Rev. A **78**, 042307 (2008).

[34] J. R. Johansson, P. D. Nation, and Franco Nori, QuTiP: An open-source Python framework for the dynamics of open quantum systems, Comput. Phys. Commun. **183**, 1760 (2012).

[35] J. R. Johansson, P. D. Nation, and Franco Nori, QuTiP 2: A Python framework for the dynamics of open quantum systems, Comput. Phys. Commun. **184**, 1234 (2013).

[36] Sanjay Moudgalya and Olexei I. Motrunich, Hilbert space fragmentation and commutant algebras, Phys. Rev. X **12**, 011050 (2022).

[37] Sanjay Moudgalya and Olexei I. Motrunich, From symmetries to commutant algebras in standard Hamiltonians, Ann. Phys. (Amsterdam) **455**, 169384 (2023).

[38] See Supplemental Material at http://link.aps.org/supplemental/10.1103/zn9v-k73w for additional information about the commutant algebra, the effective Lindbladian obtained using perturbation theory, the properties of the Markov generator $\tilde{W}$, and other models displaying the same phenomenology as the one studied in the main text. The Supplemental Material also contains Refs. [18,29,36,37,39,40].

[39] Hal Tasaki, *Physics and Mathematics of Quantum Many-Body Systems* (Springer, New York, 2020), Vol. 66.

[40] Stefan Knabe, Energy gaps and elementary excitations for certain VBS-quantum antiferromagnets, J. Stat. Phys. **52**, 627 (1988).

[41] Matthew Fishman, Steven R. White, and E. Miles Stoudenmire, The ITensor software library for tensor network calculations, SciPost Phys. Codebases 4 (2022).

[42] Matthew Fishman, Steven R. White, and E. Miles Stoudenmire, Codebase release 0.3 for ITensor, SciPost Phys. Codebases 4–r0.3 (2022).

[43] Mingru Yang and Steven R. White, Time-dependent variational principle with ancillary Krylov subspace, Phys. Rev. B **102**, 094315 (2020).

[44] Jutho Haegeman, J. Ignacio Cirac, Tobias J. Osborne, Iztok Pižorn, Henri Verschelde, and Frank Verstraete, Time-dependent variational principle for quantum lattices, Phys. Rev. Lett. **107**, 070601 (2011).

[45] Saverio Bocini and Maurizio Fagotti, Growing Schrödinger's cat states by local unitary time evolution of product states, Phys. Rev. Res. **6**, 033108 (2024).

[46] Leo P. Kadanoff and Paul C. Martin, Hydrodynamic equations and correlation functions, Ann. Phys. (N.Y.) **24**, 419 (1963).

[47] Herbert Spohn, *Large Scale Dynamics of Interacting Particles* (Springer Science & Business Media, New York, 2012).

[48] Benjamin Doyon, Lecture notes on generalised hydrodynamics, SciPost Phys. Lect. Notes 018 (2020).

[49] He-Ran Wang, Dong Yuan, Shun-Yao Zhang, Zhong Wang, Dong-Ling Deng, and L.-M. Duan, Embedding quantum many-body scars into decoherence-free subspaces, Phys. Rev. Lett. **132**, 150401 (2024).

[50] Marius de Leeuw, Chiara Paletta, Balázs Pozsgay, and Eric Vernier, Hidden quasilocal charges and Gibbs ensemble in a Lindblad system, Phys. Rev. B **109**, 054311 (2024).

[51] Víctor Fernández-Hurtado, Jordi Mur-Petit, Juan José García-Ripoll, and Rafael A. Molina, Lattice scars: Surviving in an open discrete billiard, New J. Phys. **16**, 035005 (2014).

[52] Berislav Buča, Joseph Tindall, and Dieter Jaksch, Non-stationary coherent quantum many-body dynamics through dissipation, Nat. Commun. **10**, 1730 (2019).

[53] Qianqian Chen, Shuai A. Chen, and Zheng Zhu, Weak ergodicity breaking in non-Hermitian many-body systems, SciPost Phys. **15**, 052 (2023).

[54] Adam Nahum, Jonathan Ruhman, Sagar Vijay, and Jeongwan Haah, Quantum entanglement growth under random unitary dynamics, Phys. Rev. X **7**, 031016 (2017).

[55] Tianci Zhou and Adam Nahum, Entanglement membrane in chaotic many-body systems, Phys. Rev. X **10**, 031066 (2020).

[56] Masao Doi, Stochastic theory of diffusion-controlled reaction, J. Phys. A **9**, 1479 (1976).

[57] Masao Doi, Second quantization representation for classical many-particle system, J. Phys. A **9**, 1465 (1976).

[58] Yuto Ashida, Zongping Gong, and Masahito Ueda, Non-Hermitian physics, Adv. Phys. **69**, 249 (2020).

[59] Julius T. Gohsrich, Ayan Banerjee, and Flore K. Kunst, The non-Hermitian skin effect: A perspective, arXiv:2410.23845.

[60] Federico Gerbino, Igor Lesanovsky, and Gabriele Perfetto, Large-scale universality in quantum reaction-diffusion from Keldysh field theory, Phys. Rev. B **109**, L220304 (2024).

[61] Alice Marché, Hironobu Yoshida, Alberto Nardin, Hosho Katsura, and Leonardo Mazza, Universality and two-body losses: Lessons from the effective non-Hermitian dynamics of two particles, Phys. Rev. A **110**, 033321 (2024).

[62] www.hqi.fr

[63] Phillip Weinberg and Marin Bukov, QuSpin: A Python package for dynamics and exact diagonalisation of quantum many body systems part I: Spin chains, SciPost Phys. **2**, 003 (2017).

[64] Phillip Weinberg and Marin Bukov, QuSpin: A Python package for dynamics and exact diagonalisation of quantum many body systems. Part II: bosons, fermions and higher spins, SciPost Phys. **7**, 020 (2019).

[65] Subir Sachdev, Quantum phase transitions, Phys. World **12**, 33 (1999).

[66] F. Verstraete, J. J. García-Ripoll, and J. I. Cirac, Matrix product density operators: Simulation of finite-temperature and dissipative systems, Phys. Rev. Lett. **93**, 207204 (2004).

[67] Jian Cui, J. Ignacio Cirac, and Mari Carmen Bañuls, Variational matrix product operators for the steady state of dissipative quantum systems, Phys. Rev. Lett. **114**, 220601 (2015).

[68] Sebastian Paeckel, Thomas Köhler, Andreas Swoboda, Salvatore R. Manmana, Ulrich Schollwöck, and Claudius Hubig, Time-evolution methods for matrix-product states, Ann. Phys. (Amsterdam) **411**, 167998 (2019).

[69] Jutho Haegeman, Christian Lubich, Ivan Oseledets, Bart Vandereycken, and Frank Verstraete, Unifying time evolution and optimization with matrix product states, Phys. Rev. B **94**, 165116 (2016).

[70] Naomichi Hatano and David R. Nelson, Localization transitions in non-Hermitian quantum mechanics, Phys. Rev. Lett. **77**, 570 (1996).

[71] V. M. Martinez Alvarez, J. E. Barrios Vargas, and L. E. F. Foa Torres, Non-Hermitian robust edge states in one dimension: Anomalous localization and eigenspace condensation at exceptional points, Phys. Rev. B **97**, 121401(R) (2018).

[72] Shunyu Yao and Zhong Wang, Edge states and topological invariants of non-Hermitian systems, Phys. Rev. Lett. **121**, 086803 (2018).

## End Matter

*Commutant algebra*—We discuss the properties of the commutant algebra (reviewed in [36,37]) associated with the model in Eq. (1) of the main text. Such analysis is particularly useful for open quantum systems, as shown in Ref. [21], since it allows us to identify in general a set of (both local and nonlocal) symmetries associated with the terms appearing in the Lindbladian for a generic choice of the couplings. For instance, given the Hamiltonian $H = \sum_j h_j$ and the local dissipators $L_j$, one defines the commutant algebra $\mathcal{C}$

$$\mathcal{C} := \{\mathcal{O} | [\mathcal{O}, h_j] = [\mathcal{O}, L_j] = [\mathcal{O}, L_j^\dagger] = 0 \quad \forall \ j\}. \tag{A1}$$

We observe that the dissipators of (1) are Hermitian, $L_j^\dagger = L_j$, and both 1 and $|\Uparrow\rangle\langle\Uparrow|$ belong to $\mathcal{C}$. Specifically, one can show that $\mathcal{C} = \mathrm{Span}\{1, |\Uparrow\rangle\langle\Uparrow|\}$, meaning that these operators generate the entire commutant algebra. We sketch the proof here: (i) Since we are interested in $g, J \neq 0$ being generic, we will focus on operators that commute with both the hopping and the East-West term in the Hamiltonian. (ii) We identify the operators that commute with $\sigma_j^z, \sigma_{j+1}^z, (1 - \sigma_j^z)\sigma_{j+1}^x, (1 - \sigma_{j+1}^z)\sigma_j^x$ at a given position $j$. One can check that these also commute with $\sigma_j^+\sigma_{j+1}^- + \sigma_j^-\sigma_{j+1}^+$. (iii) Finally, one intersects progressively the spaces of operators introduced above over the site index $j$.

The result of this procedure, which can be obtained using induction over the length of the chain, gives precisely $\mathrm{Span}\{1, |\Uparrow\rangle\langle\Uparrow|\}$.

As a final remark, we point out that, for specific choices of the couplings, as for example $g = 0$ (where $\sum_j \sigma^z$ is conserved), additional symmetries can be present and the commutant algebra becomes larger: we consider that as a fine-tuning. In particular, since $\mathcal{C} \subseteq \ker \mathcal{L}$ [from the definition (A1)] and a double degeneracy of the zero eigenvalue is observed at $g, J \neq 0$ (that is, $\ker \mathcal{L} = \mathrm{Span}\{1, |\Uparrow\rangle\langle\Uparrow|\}$), one safely concludes that $\mathcal{C} = \mathrm{Span}\{1, |\Uparrow\rangle\langle\Uparrow|\}$. Additional details are given in SM [38].

*Spectral properties of the Lindbladian*—Here, we discuss the spectral properties of the Lindbladian in Eq. (1). We first, summarize the main steps to obtain the effective Markov generator $W$ in Eq. (5), in the limit of small $g/\gamma, J/\gamma$. The method is based on second-order perturbation theory on the Lindbladian, and it has been employed in [18].

(i) One first identifies the spectrum of the dissipator, found for $g, J = 0$ in Eq. (1). An explicit calculation shows that matrix elements of the form $|\boldsymbol{\sigma}\rangle\langle\boldsymbol{\sigma}'|$, with $\boldsymbol{\sigma}, \boldsymbol{\sigma}'$ spin configurations in the $z$-direction, are eigenvectors and their eigenvalue is proportional to the number of mismatches between $\boldsymbol{\sigma}$ and $\boldsymbol{\sigma}'$. (ii) In particular, in the absence of perturbation, the manifold of stationary states, associated with $\lambda = 0$, is generated by the diagonal elements $|\boldsymbol{\sigma}\rangle\langle\boldsymbol{\sigma}|$. For small $g, J \neq 0$, the large degeneracy of the Lindbladian is lifted and, at the lowest order, the effective couplings between unperturbed eigenvectors are given by virtual transitions onto unperturbed eigenspaces. (iii) Specifically, from the effective couplings between the diagonal elements $|\boldsymbol{\sigma}\rangle\langle\boldsymbol{\sigma}|$, one can identify an effective Lindbladian which describes the low spectrum of $\mathcal{L}$ (and having the same matrix elements of $-W$). This allows us to reduce the complexity of diagonalizing a $4^L \times 4^L$ matrix, associated with $\mathcal{L}$, to the diagonalization of a $2^L \times 2^L$ matrix, corresponding to $W$, as far as the low-spectrum is concerned.

The explicit calculations to obtain the expression of $W$ are straightforward but lengthy, and they are reported in SM [38]. As a by-product, we perform a numerical check and we compare the spectrum of $\mathcal{L}$ and that of $-W$ obtained via exact diagonalization using the open-source Python package QuSpin [63,64]; in Fig. 5 we show the results for $L = 4$, with $[g, J, \gamma] = [0.5, 0.5, 100]$.

We now discuss the properties of the lowest energy states of the Markov generator above the ground state manifold. First, we observe that $W \geq 0$ and has $|\Uparrow\rangle$ and $|\Rightarrow\rangle$, with every spin aligned along the $z$ and $x$ axis, respectively, as exact eigenstates with vanishing energy (corresponding with the exceptional stationary state and the infinite temperature state, belonging to the kernel of the Lindbladian). Being this operator gapped, as shown numerically in Fig. 1, one expects that its first excited states correspond to domain-wall excitations, interpolating between the two ground states, at given momenta (a property that we found analytically, using the techniques introduced in Refs. [39,40], for the simplified model $\tilde{W}$ introduced in the main text): while this is formally correct for infinite systems, carefulness is needed for finite systems, and the choice of boundary conditions plays a role. For instance, while a single domain wall can be present with open boundary conditions, only an even number of them can be hosted in the periodic chain: this is analogous to the properties of the spectrum of the quantum Ising chain [65]. As a consequence, the origin of the spectral gap is traced back to a one- or two-domain
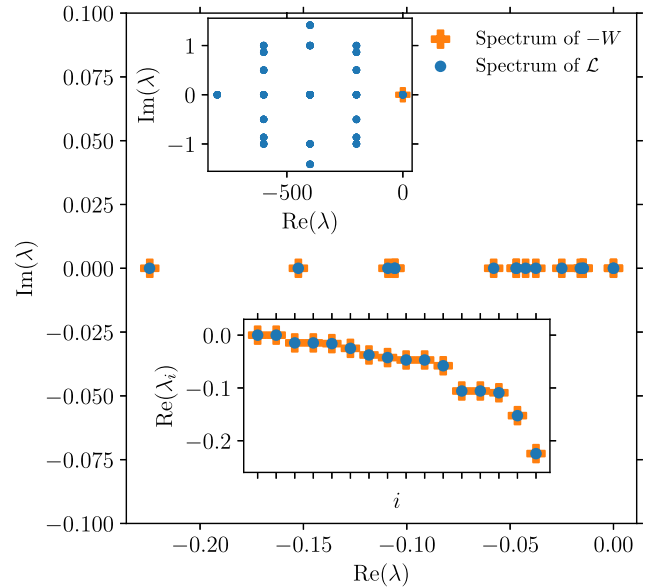


FIG. 5. Comparison between the slow decaying modes of the Lindbladian $\mathcal{L}$ and the spectrum of the effective Hamiltonian $-W$. The parameters are $[J, g, \gamma, L] = [0.5, 0.5, 100, 4]$. In the top inset, the full spectrum of $\mathcal{L}$ is represented. In the bottom inset, we show the real part of the slow decaying modes labeled by the index $i$.
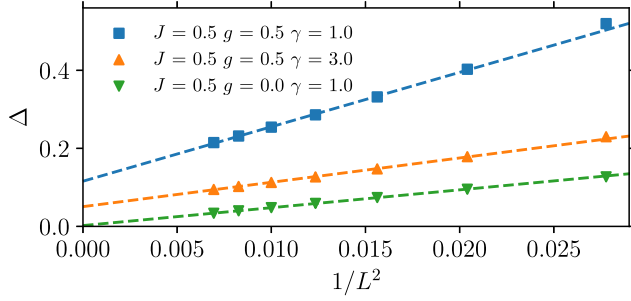
FIG. 6. Lindbladian gap $\Delta$ as function of $1/L^2$ for $L \in \{6, \ldots, 12\}$ and periodic boundary conditions.

wall excitation with the lowest possible momenta (allowed from the quantization induced by the boundary conditions), for the open/periodic chain, respectively. While the previous discussion refers to the Markov generator, we expect that similar properties holds for the Lindbladian. In particular, a discrepancy between the spectral gap with the two aforementioned boundary conditions is explicitly observed: in Fig. 6 we show the results with periodic boundary conditions, that have to be compared with those in Fig. 1.

*Details on the tensor-network numerical computations*— Here, we give some details on the implementation of the tensor-network numerical simulations. We vectorize the density matrix $\rho$, as done in Refs. [66,67]. In this representation, the Lindbladian $\mathcal{L}$ becomes a linear operator. We represent the vectorized $\rho$ as a matrix-product state and $\mathcal{L}$ as a matrix-product operator. The time evolution is performed using the time-dependent variational principle (TDVP) [44,68,69]. In this way, we are able to simulate chains of $L = 40$ sites up to time $t = 30$ for $[J, g, \gamma] = [0.5, 0.5, 1]$. The bond dimension, the number of sweeps and the time step used in all this Letter are $\chi = 200$, $n_{\text{sweeps}} = 5$, and $\delta t = 0.1$, respectively.

*On the exponential loss of coherence between $\mathcal{S}_\Uparrow$ and $\mathcal{T}_\Uparrow$*—We discuss here the exponential loss of coherence between $|\Uparrow\rangle$ and the states orthogonal to it, expressed by the quantity $\eta(t)$ in Eq. (4). To study its behavior, we consider the evolution of $\langle\boldsymbol{\sigma}|\rho(t)|\Uparrow\rangle$, with $|\boldsymbol{\sigma}\rangle \neq |\Uparrow\rangle$. A simple calculation, starting from Eq. (1) gives

$$\frac{d}{dt}\langle\boldsymbol{\sigma}|\rho(t)|\Uparrow\rangle$$
$$= \langle\boldsymbol{\sigma}| -i[H, \rho(t)] + \gamma\sum_j (\sigma_j^z \rho(t)\sigma_j^z(t) - \rho(t))|\Uparrow\rangle. \quad (D1)$$

Using $H|\Uparrow\rangle = 0$ and $\sigma_j^z|\Uparrow\rangle = |\Uparrow\rangle$, we express

$$\frac{d}{dt}\langle\boldsymbol{\sigma}|\rho(t)|\Uparrow\rangle = -\sum_{|\boldsymbol{\sigma}'\rangle \neq |\Uparrow\rangle}\langle\boldsymbol{\sigma}|K|\boldsymbol{\sigma}'\rangle\langle\boldsymbol{\sigma}'|\rho(t)|\Uparrow\rangle \quad (D2)$$

with $K = iH + \gamma\sum_j(1 - \sigma_j^z)$. In other words, the evolution of $\langle\boldsymbol{\sigma}|\rho(t)|\Uparrow\rangle$, seen as a column vector with entries parametrized by $\boldsymbol{\sigma}$, is ruled by the matrix $K$. We observe that $K + K^\dagger = 2\gamma\sum_j(1 - \sigma_j^z)$, and therefore the eigenvalues of $K + K^\dagger$ are $\geq 4\gamma$ in the subspace orthogonal to $|\Uparrow\rangle$. As a consequence, the entries of $\langle\boldsymbol{\sigma}|\rho(t)|\Uparrow\rangle$ are expected to decay exponentially with a rate proportional to $\gamma$. A quantitative estimate can be provided for the quantifier $\eta(t)$ and, after straightforward algebra, we obtain

$$-\frac{d}{dt}\eta(t) = \langle\Uparrow|\rho(t)(K + K^\dagger)\rho(t)|\Uparrow\rangle \geq 4\gamma\eta(t), \quad (D3)$$

which implies $\eta(t) \leq e^{-4\gamma t}\eta(0)$.

*Finite-size matrix elements of $\tilde{W}$ and non-Hermitian skin effect*—We discuss the matrix elements entering Eq. (9). We first remark that the space of 1-domain wall configurations is closed under time evolution induced by $\tilde{W}$; thus, it is sufficient to project $\tilde{W}$ onto the associated sector, of dimension $L$, and diagonalize the resulting $L \times L$ matrix. Its diagonalization can be performed efficiently, as it reduces to a single-particle problem with open boundary conditions.

A similar problem appears in the Hatano-Nelson model [70], which is a non-Hermitian free fermionic chain; there, the imbalance between the left and right hopping rate is known to result in the localization of the eigenfunctions, a mechanism known as *non-Hermitian skin effect* [71,72]. The same phenomenology is found in our model and, in particular, we have checked that the right/left eigenfunctions are localized around the right/left boundary respectively. This is sufficient to explain the exponential growth of the matrix elements in Eq. (9), as we explain below.

Let us consider a simple ansatz $(x|n) \propto e^{-\tilde{k}(L-x)}$, $(\tilde{n}|x) \propto e^{-kx}$ with $k$ a complex number (depending on $n$) satisfying $\text{Re}(k) > 0$. We focus on an observable with support on the right of $x_0$, choosing for simplicity $\mathcal{O} = |x)(x|$, corresponding to the probability distribution of the interface at position $x$. We estimate

$$(\mathbb{1}|\mathcal{O}|n)(\tilde{n}|x_0) \simeq \frac{e^{-k(L-x)}e^{-kx_0}}{\sum_{x'}e^{-k(L-x')}e^{-kx'}} \sim \frac{e^{k(x-x_0)}}{L}, \quad (E1)$$

where the denominator comes from the normalization condition $(\tilde{n}|n) = 1$. As a consequence, if $x - x_0 \sim L$ the absolute value of Eq. (E1) is exponentially large in $L$.

Finally, we point out that while the sum in Eq. (8) converges in the thermodynamic limit, the corresponding sum of the absolute values in Eq. (9) diverges exponentially in $L$. The origin of this discrepancy can be traced back to the phases of the matrix element (E1), which are highly oscillating as functions of $n$.